Dynamos and Outflows in Simulations of Protostellar Collapse

Nathan Goldbaum
Department of Astronomy & Astrophysics
University of California, Santa Cruz

ABSTRACT

We present simulations of the collapse of a massive rotating protostellar core assuming conditions characteristic of Population III star formation. Starting with an initially weak magnetic field, we find that the combined action of compression and dynamo processes amplify the field to nearly equipartition levels. At late times, we find the magnetic field is able to buoyantly rise above and below the protostellar disk, producing a large-scale magnetic field.

1. Introduction

In the local universe, star formation is regulated by magnetic fields. While magnetic fields are not energetically dominant in the dynamics of a molecular cloud core (Crutcher, 1999), even a moderately strong magnetic field is sufficient to halt the formation of a Keplerian disk when one assumes perfect flux freezing (Mellon & Li, 2008). Although non-ideal effects are expected to allow the formation of a Keplerian accretion disk (Mellon & Li, 2009), one must still take into account the effects of an initially strong magnetic field when attempting to understand the collapse of protostars and the formation of protoplanetary disks.

Such is not the case when considering the formation of the first stars. In this regime, stars are thought to have formed via the gravitational collapse of massive cores permeated by a very weak magnetic field. This field may have initially been seeded by quantum effects during the Big Bang, and then amplified by the Biermann (1950) battery effect (Xu et al., 2008).

Today, dynamically important magnetic fields are universally observed. The origin of these fields is unknown and explaining the generation of so much magnetic energy in the universe is a challenging unsolved problem (Carilli & Taylor, 2002). These fields, particularly on the largest scales, may have been seeded by magnetic fields generated in the collapse of the first stars and then amplified via dynamo processes. Simulations of comsmic structure formation including the Biermann battery effect find that the initial conditions for Population III star formation must begin with a weak field, with $\beta = P_{\rm gas}/P_{\rm mag} \gtrsim 10^{15}$ (Xu et al., 2008).

Sur et al. (2010) and Federrath et al. (2011) simulated the collapse of an isolated gravitationally unstable Bonnor-Ebert sphere with an initially weak magnetic field ($\beta \approx 10^{10}$). Following the collapsing Jeans volume up to a density of $n \lesssim 10^{10}$ cm^{-3}, these authors found that turbulence in the initial conditions along with turbulent motions generated as the core gravitationally collapses power a dynamo sufficient to produce a dynamically important magnetic field within the collapsing volume.

These studies focused on small scales, within the Lagrangian parcel of gas that would eventually collapse and form the protostar. Thus, they could only draw conclusions about the production of magnetic fields within the gas that would eventually collapse to stellar densities. Since the collapse was not cut off at some limiting scale, the large-scale dynamics of the protostellar core were essentially frozen at the moment of protostellar ignition. For this reason, they could not make conclusions about the production of large scale fields, as large-scale fields can only be amplified on the much slower dynamical timescales outside the collapsing region. Here, we use a similar setup to that of Sur et al. (2010) and Federrath

et al. (2011), but instead focus on the formation and long-term evolution of the protostellar core. We also impose a nonzero initial net angular momentum to encourage the formation of a protostellar disk.

Below, we show how our simulations produce a dynamically important, large-scale magnetic field through a disk dynamo. We also report on the large-scale state of the magnetic fields in the protostellar disk and envelope. We discuss the launching of a magnetocentrifugal outflow in the last stages of the protostellar collapse, a mechanism that might limit the final mass of the forming protostar. We first discuss the setup of our simulations in Section 2. Next, in Section 3 we discuss the dynamo process we observe in our simulations. This is followed by a discussion in Section 4 of the outflows we observe at late times in our simulations.

2. Methods

We model the gravitational collapse of a turbulent, gravitationally unstable protostellar core via high-resolution numerical simulations. Our calculations were performed with version 2.5 of the FLASH code (Fryxell et al., 2000). We evolve the equations of ideal magnetohydrodynamics (MHD), including self-gravity. We take advantage of the adaptive mesh refinement (AMR) capabilities of the FLASH code, and require that the Jeans length,

$$\lambda_J = \left(\frac{\pi c_s^2}{G\rho}\right)^{1/2} \tag{1}$$

where c_s is the sound speed, G is the gravitational constant, and ρ is the gas density, always be resolved by a user-defined number of cells. As described in Federrath et al. (2011), we use the HLL3R approximate Riemann solver to efficiently and accurately evolve the equations of ideal MHD.

The initial conditions and thermodynamics of our simulation is motivated by high-resolution 'zoom-in' simulations of the formation of the first stars (Abel et al., 2002; Yoshida et al., 2008; Clark et al., 2011). The initial conditions are that of a Bonnor-Ebert sphere of dimensionless radius $\xi = 8.28$ and temperature $T = 300$ K, corresponding to a physical radius of $R_{\rm core} = 1.5$ pc, mass $M_{\rm core} = 1250 M_\odot$, and central density $\rho_0 = 4.68 \times 10^{-20}$ g cm^{-2}. For comparison, the Jeans length and mass at a temperature of 300 K and a density of $\rho = \rho_0$ are $\lambda_J = 0.84$ pc and $M_J = 1700 M_\odot$. Since the density distribution is stratified rather than uniform, the characteristic mean density is somewhat lower than the estimate used above, implying the true Jeans length and mass are somewhat longer and lower, respectively. Thus, our initial conditions contain approximately one Jeans volume that will collapse and form a single, massive protostar. Detailed simulations of the coupled hydrodynamics, thermodynamics, and chemodynamics of primordial gas collapsing to produce the first star find that the gas satisfies a polytropic equation of state with a slope $\Gamma = 1 + d\ln P/d\ln\rho = 1.1$ in the density range we are interested in. We approximately include this physics by imposing a polytropic EOS on the gas. Since the cooling time is short compared to the dynamical time, this is an excellent approximation.

We give the gas some initial rotation, such that the ratio of the rotational energy to the gravitational binding energy,

$$\beta = \frac{(1/2)I\Omega^2}{aGM_{\rm core}^2/R_{\rm core}} \tag{2}$$

is about 7% in the initial conditions. Applying the impulse approximation, we thus expect the gas to circularize at a characteristic radius $r_{\rm min} = R_{\rm core}^4\Omega^2/GM_{\rm core} \approx \beta R_{\rm core}$, to a within a factor of order unity.

The velocity structure of the core is initialized with transonic $\mathcal{M} = 1$ turbulence, corresponding to RMS velocity dispersion, $(\langle v \rangle^2)^{1/2} = 1.1$ km s^{-1}. The turbulence is initialized by drawing from a power spectrum $P(k) \propto k^{-2}$, with power allocated between a minimum and maximum wavenumber $k_{\rm min} = 1$ and $k_{\rm max} = k_{\rm Nyquist}$. Power injected at wavenumbers below $k = \pi$ is undersampled and the turbulent power spectrum is not proportional to k^{-2} between $k_{\rm min}$ and $k = \pi$. The magnetic field if initialized in an analogous way by drawing from a different realization drawn from the same power spectrum. The magnetic field has an rms strength, $B_0 = 1\mu$G, corresponding to an initial RMS plasma β, $\beta_0 \approx 10^4$. This is a somewhat stronger magnetic field than was used in Sur et al. (2010) and Federrath et al. (2011), however, this choice does not effect the character of the collapse, and only makes a difference late in the evolution of the disk. In both cases, fields become dynamically important, but only after a delay for the $B_0 = 1$nG case. For this preliminary study, we chose to use an initial magnetic field 10^3 time stronger to avoid simulating the ramp-up phase for a prohibitively long period of time.

So as to understand the dependence of our results on numerical resolution, we have performed a set of five simulations, varying the parameters controlling the resolution. Since our simulations use an AMR code, our ability to resolve the formation and evolution of a disk is set by the maximum refinement level, l_{max} and jeans resolution parameter, $J = \Delta x/\lambda_J$ where Δx is the grid spacing at a given refinement level. In studies of gravitational instability in the hydrodynamic limit, studies normally point to the Truelove et al. (1997) criterion, requiring that the Jeans length be resolved by a minimum of 4 grid cells (J = 0.25) at all times to prevent artificial fragmentation. While this is still true in the magnetohydrodynamic case, Federrath et al. (2011) shows that one must resolve the Jeans length with a minimum of 30 cells (J = 0.033) to ensure that artificial dissipation of magnetic energy at the grid scale is small enough to allow the development of a turbulent dynamo and a corresponding exponential increase in the magnetic energy with time. Since we expect that dynamo processes will be important in our simulation, we explore three choices for the Jeans resolution, $J = 0.0625, 0.03125,$ and 0.015625, corresponding to $16, 32,$ and 64 cells per Jeans length, respectively. At the same time, we can vary the maximum refinement level. This allows us to better resolve high density gas in the inner region of the accretion disk. We have run simulations with $l_{\rm max} = 9, 10,$ and 11. This is defined such that the base, $l = 0$, grid consists of a 4^3 grid of cells encompassing the entire computational domain ($\Delta x = 3.9$ pc). Our reference simulations is evolved with $J = 0.03125$ and $l_{\rm max} = 10$. The initial conditions are refined to satisfy the Jeans resolution criteria, implying that the initial conditions in our reference run have already refined to $l = 6$, leaving four further levels of refinement before collapse proceeds to the point where the Jeans length is no longer resolved.

So that we resolve the evolution of the disk beyond the point where we will break the Jeans resolution criterion, we employ the Lagrangian sink particle prescription of Federrath

et al. (2010). Once the gas collapse reaches the maximum refinement level l_{max}, and the Jeans resolution criterion is locally violated, $\lambda_J \leq \Delta_x/J$ for some grid cell on the maximum refinement level, the gas is transferred from the grid to a Lagrangian sink particle. The sink accretes gas in such a manner to ensure that the imposed jeans resolution criterion is always satisfied and self-consistently prevents triggering of refinement beyond l_{max}. Sink creation and accretion follow the standard recipes of Bate et al. (1995), with modifications to account for the energy content of magnetized gas as described by Federrath et al. (2010). In this prescription, a sink is only created if the gas is above a maximum resolvable density,

$$\rho_{\rm max} = \left(\frac{\pi c_{s,0}^2}{4 G r_{\rm acc}^2 \rho_0^{\Gamma-1}} \right)^{1/(2-\Gamma)} \tag{3}$$

where $r_{\rm acc}$ is the maximum distance a parcel of material can be from the sink if it can be accreted onto the sink particle, and the gas is gravitationally bound to prevent the formation of spurious sinks in unbound gas at the vertices of shocks (see Krumholz et al. (2004) for an alternative approach). No special boundary condition is imposed on the magnetic field at the sink particle. In practice, this means that gas can be transferred off of the grid to the sink particle but magnetic flux cannot. As described by Cunningham et al. (2011, in prep), this can lead to the release of outward propagating magnetosonic waves as matter is accreted onto a sink, releasing the magnetic flux that was trapped in the accreted parcel of gas.

So that our sinks have a consistent size as a function of numerical resolution, we fix $r_{\rm acc} = 780$ AU, corresponding to a maximum resolvable density $n_{\rm max} = 6.93 \times 10^{-16}$ g cm^{-3}. The accretion radius is therefore resolved by four cells in the reference simulation. Therefore, in the lowest resolution simulation, the sink control region is resolved by four cells (i.e. $r_{\rm acc} = 2\Delta x$ at $l = l_{\rm max}$), consistent with the minimum resolution requirements for sink particles in earlier studies (Federrath et al., 2011). This limits the dynamic range in overdensity in our simulations to a factor of $\sim 10^4$, and only allows us to resolve the outer region of the accretion disk.

3. Disk Dynamo

Here we discuss the gross morphological features of our simulations as well as the amplification of the magnetic field we observe after the formation of the protostar. As described above, the initial conditions of our simulations are seeded with a weak, turbulent magnetic field and a transonic turbulent velocity field. Since the magnetic field is initially quite weak, the Lorentz force is negligible at early times. In this regime, the cloud experiences a decay of turbulence over approximately a dynamical time, $t_{\rm cr} = R_{\rm core}/(\langle v^2 \rangle)^{1/2} = 3.5 \times 10^6$ years. Since the core is centrally condensed, collapse actually proceeds approximately 50% faster than this rough estimate would suggest. Once the turbulence decays away, collapse proceeds over the comparatively quicker free-fall timescale $t_{\rm ff} = (3\pi/32 G \rho_0)^{1/2} = 3.1 \times 10^5$ years.

Once a protostar forms at the center of the collapsing core, a disk begins to form, with a characteristic radius consistent with the rough estimate derived above, $r_{\rm min} = \beta R_{\rm core} = 3 \times 10^4$ AU. Once a disk forms, any evolution must occur on the only natural timescale in the problem, the Keplerian dynamical time,

$t_{\rm orb} = (a^3/GM_*)^{1/2} = 1.1 \times 10^4$ years $(a/10^4$ AU$)^{3/2}$ $(M_*/200\ M_\odot)^{-1/2}$ for a parcel of gas with semimajor axis a orbiting a star of mass M_*. Accounting for the finite mass of the disk would only introduce an order-unity correction to this estimate.

As the collapse proceeds and the gas density increases in the neighborhood of the protostar, the magnetic field also increases. Assuming perfect flux-freezing with no dynamo action in a spherical collapse, the magnetic field strength should scale with the gas density as $\rho^{2/3}$. Taking the central density of the Bonnor-Ebert sphere as typical of the initial conditions and comparing to the sink creation density, we thus expect to produce an RMS field at the 10^{-4} Gauss level due to pure compression. This would correspond to a typical plasma-β of order ~ 10 in the neighborhood of the sink particle.

In Figure 1, we present the evolution of the total magnetic energy in the simulation volume as a function of time for three different runs with varying Jeans resolution. One can see that there are three stages of collapse. For approximately 2.3 to 2.5 Myr, the core evolves in quasi-steady-state as the turbulence in the initial conditions decays away. In this stage, the total magnetic energy in the box does not evolve with time. This is expected as any random turbulent compression should also be accompanied by rarefaction. In the low resolution run, dissipation of magnetic energy at the grid scale reduces the magnetic energy by almost an order of magnitude before collapse sets in. In the higher resolution runs, dissipative losses are smaller, and the magnetic energy does not change very much before the collapse sets in. Collapse occurs at different times in the three simulations for the same reason, since turbulent kinetic energy is also being lost at the grid scale at varying rates

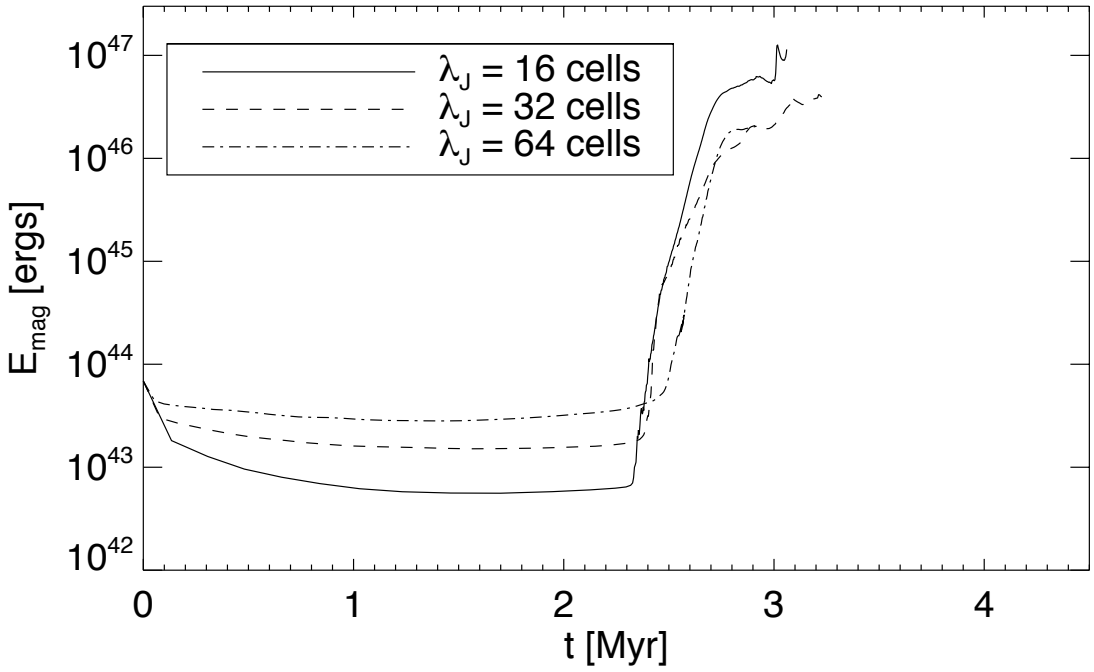

Fig. 1.— The magnetic energy contained in the simulation domain as a function of time. The evolution of simulations with $J = 0.0625, 0.03125,$ and 0.015625 are depicted as indicated in the legend.

in the three simulations. However, once collapse sets in, the magnetic energy increases by approximately three and a half orders of magnitude in all three simulations. The rate of growth and saturation level are approximately the same in all three runs. Since all three simulations were run to the same maximum refinement level, the resulting disks are all at the maximum refinement level. The Jeans resolution thus does effect the evolution of the magnetic and turbulent properties of the disk.

Once a sink particle forms, which happens in the reference simulation at $t = 2.42$ Myr, the growth of the magnetic field slows somewhat as the bulk of the gas compression has already occurred. At the same time, a rotationally supprted disk begins to form. The radius of the disk slowly increases with time, but reaches steady state at a radius consistent with the simple estimate given above, $r_{\rm disk} = 3 \times 10^4$ AU. Shortly after the formation of the disk, it is massive and self-gravitating, showing intermittent spiral structure typical of Toomre-unstable disks (Kratter et al., 2010). Tantalizingly, the magnetic field structure is shows strong deviations in the neighborhood of spiral shocks. In Figure 2, we show the column density and density-weighted magnetic field in the disk misplane $t = 2.55$ Myr, shortly after the formation of the disk. The magnetic field is primarily toroidal and remains

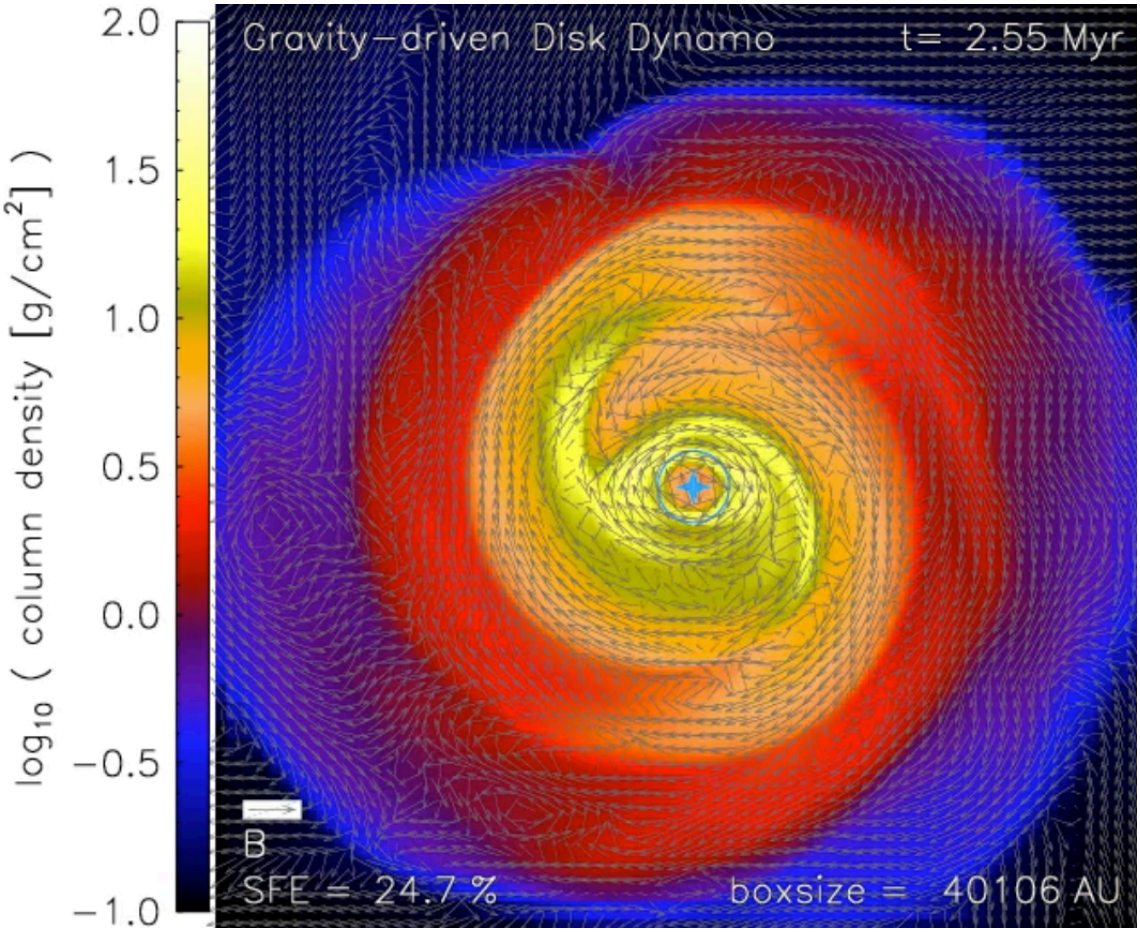

Fig. 2.— The column density and magnetic field structure of gas plane of the protostellar disk a few periods after the formation of the protostar. The vectors depict the density-weighted mean magnetic field strength in the plane of the disk. The length of a vector is logarithmically proportional to the strength of the magnetic field. Regions of magnetic field reversal are correlated with the enhanced densities in spiral shocks.

so for the rest of the simulation. The field can be aligned or anti-aligned with the flow, depending on the distance from the protostar. Movies of the evolution of the magnetic field and density structure show that the field can switch alignment during a spiral-arm passage. It is during this stage that most of the magnetic energy in the simulation is generated. The strong, dynamically important toroidal field produces regions of the disk where the magnetic pressure is comparable to the gas pressure, as can be seen in Figure 3.

As discussed above, the magnetic field amplification seems to be driven by physical processes in the protostellar disk. Since we suspect that a dynamo may be operating, we have checked whether the magnetic field amplification is a function of how well-resolved the disk is. This is because the growth rate of the magnetic field should scale with the magnetic Reynolds number $R_m = l\sigma_v/\eta$, where l is a typical length scale, σ_v is the turbulent velocity dispersion, and η is the magnetic diffusivity. Since we include no explicit magnetic diffusivity but do have implicit diffusivity due to grid effects, we can control the Reynolds

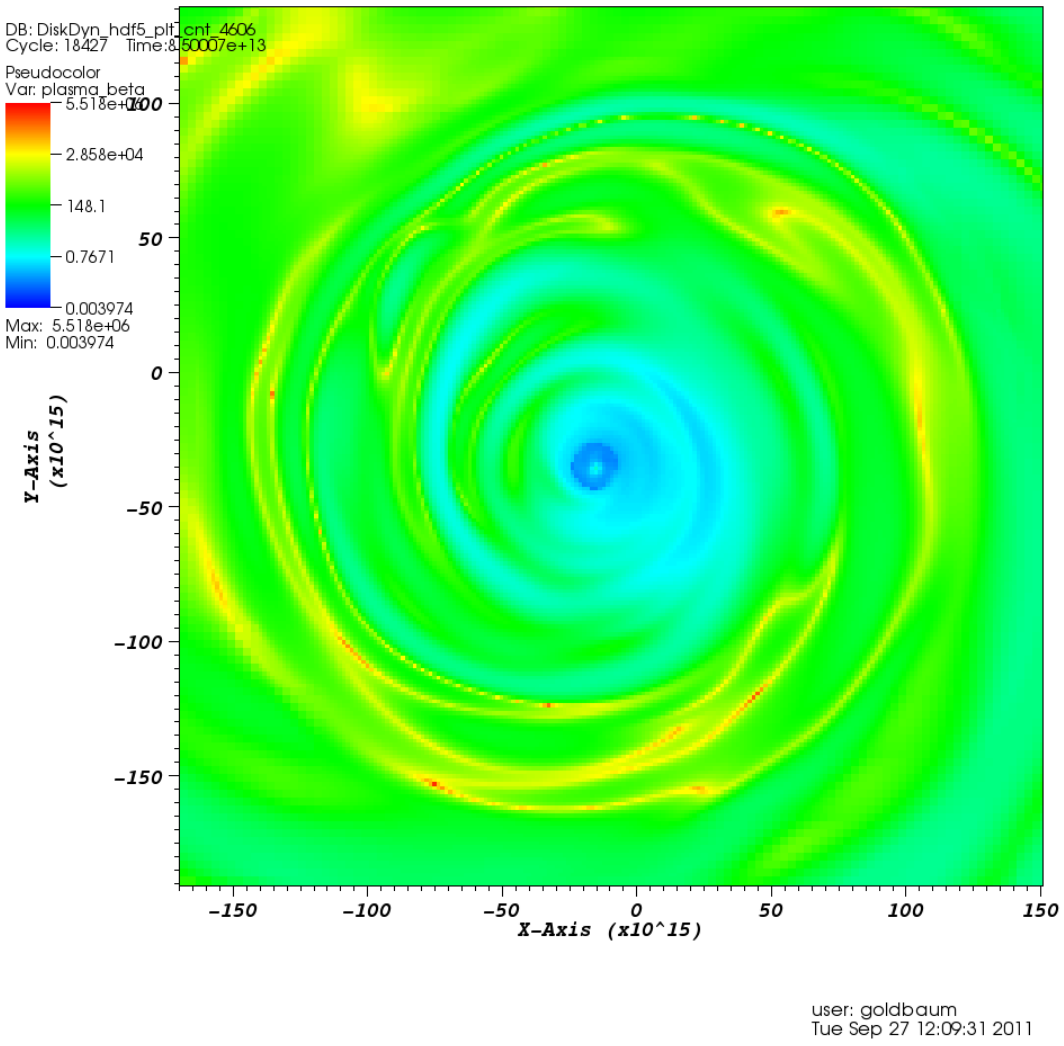

Fig. 3.— The plasma-β in the plane of the disk at $t = 2.7$ Myr in the reference simulation. The disk has developed a dynamically important magnetic field in the inner regions.

number by varying the numerical resolution. Since the inner portions of the disk, where the dynamical times are shortest and the magnetic fields are strongest, are always the maximum refinement level irrespective of how well the Jeans length is resolved, we instead use simulations with varying maximum refinement levels to study the effect of varying R_m. Varying the maximum refinement level allows us to resolve higher densities, and finer, more segmented structures within the disk.

In Figure 4, we show the evolution of the magnetic energy within the simulation box as a function of maximum refinement level. The initial evolution, before the turbulence present in the initial conditions has decayed away is identical to the $\lambda_J = 32$ cells run shown in Figure 1. In each run, the growth in the magnetic energy with time is at first driven by compression. The disk forms shortly before $t = 2.5$ Myr, and the magnetic energy grows somewhat less quickly. Afterwards, the growth of the magnetic field is driven by processes in the disk. We see that the growth rate of the magnetic field is an increasing function of resolution. After about $t = 3.0$ Myr, the main accretion phase onto the disk has completed, and most of gas has been evacuated from the envelope and fallen onto the disk. At this point, the growth of the magnetic field slows, but does not stop. This stage is only well-resolved in the low resolution simulation. The reference run and high resolution simulation has not had time to reach the saturation stage.

4. Outflows

Once the gravitational instability stage has finished, the disk reaches a quasi-steady-state configuration. The density distribution in the disk becomes smoothly stratified,

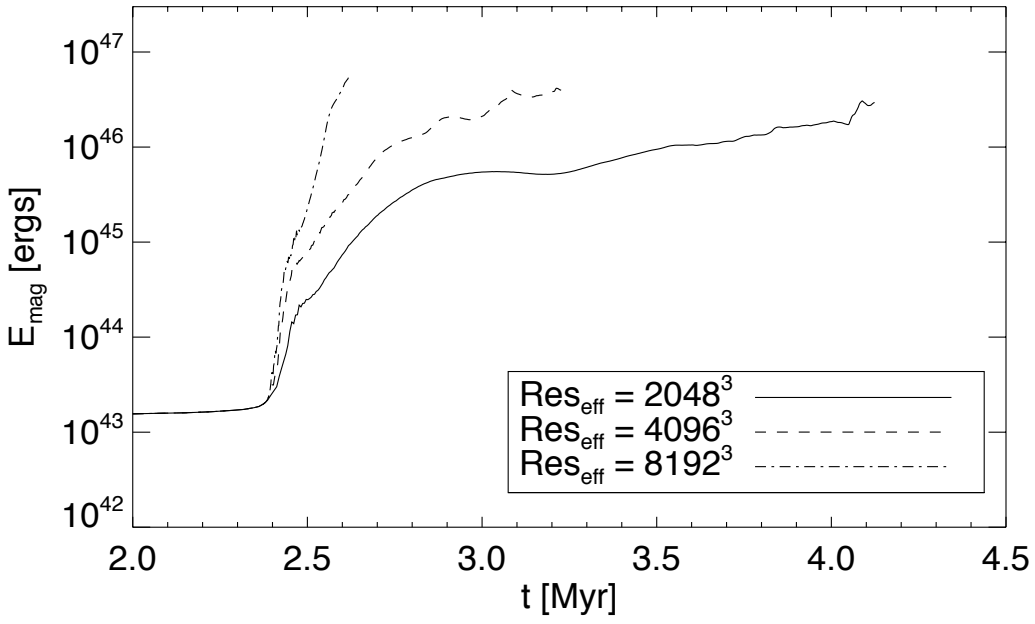

Fig. 4.— The growth of the magnetic energy in three simulations run with increasing maximum refinement level and correspondingly decreasing magnetic Reynolds number. Simulations run at higher resolution develop a stronger magnetic field than simulations run at low resolution.

showing few nonaxissymmetric features. The magnetic field structure is somewhat more complex. While the field is primarily toroidal, the orientation of the field flips at discrete radii. At any fixed radius, the orientation of the magnetic field flips somewhat randomly as material is advected through the disk onto the protostar. This may be due to the fact that the initial magnetic field had most of its power at large scales. The orientation of the magnetic field at some radius therefore corresponds to the orientation in the sign of the net magnetic flux in the initial conditions associated with material in the disk at any given radius. Since flux is conserved, this material maintains the sign of the flux as it collapses into the disk. The orientation flips at discrete intervals due to their being a finite number of turbulent eddies, each with a random positive or negative flux in the initial conditions.

Regardless of the detailed state of the magnetic field in the protostellar disk, the global state of the simulations consists of two components. The first consists of the protostellar disk, a region with a strong magnetic field, high density and thus high gas pressure, and very little vertical motion. The second region is the low-density envelope, a region with a comparatively weak magnetic field falling onto the disk at approximately the escape velocity, and thus bearing significant ram pressure. This configuration is susceptible to the magnetic bouyancy instability (e.g. Cunningham et al. 2011, in prep), producing a region above and below the disk with strong magnetic field. At first, this region is compressed by the ram pressure of the accretion flow. Eventually, the accretion rate declines, and the ram pressure falls below the magnetic pressure, allowing magnetic field lines to buoyantly rise above and below the disk. This process does not happen in synchrony for both the top and bottom half of the disk, as can be seen in Figure 5. At this point in the simulation, the accretion from the bottom half of the core is still sufficient to prevent the magnetic dominated region below the disk from expanding outward. On the top half, however, the accretion rate has slowed, and a magnetic buoyant bubble has begun to rise above the disk, carrying off a small amount of mass away from the disk. At late times, we see periodically expanding shells bounded by magnetosonic waves. These shells reduce the accretion rate onto the protostar and also carry the magnetic field produced in the disk to regions above and below the protostar.

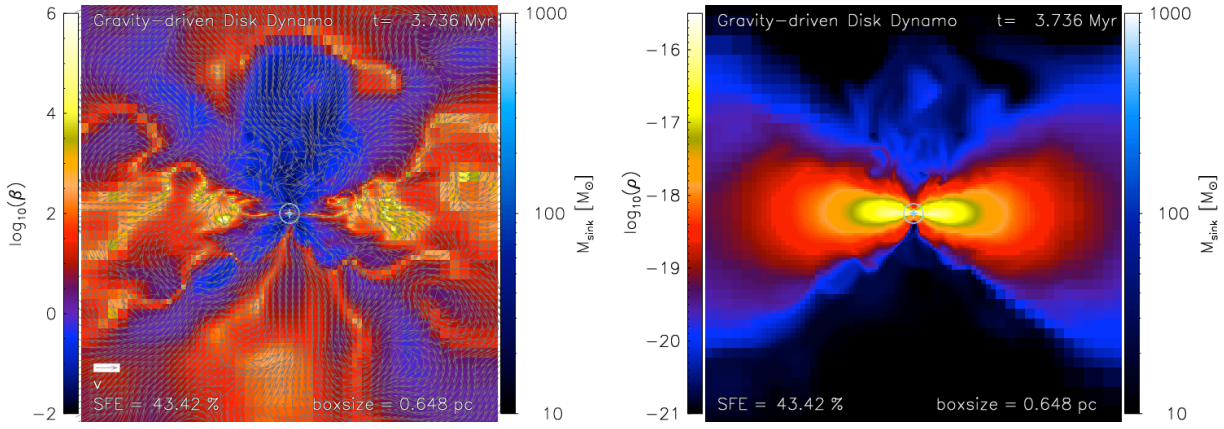

Fig. 5.— The magnetic structure (left), indictated by the plasma-β in a vertical slice throug the disk and density structure (right) in the same slice. The arrows in the left-hand plot indicate the velocity field in the same manner as the magnetic field in Figure 2.

5. Conclusions

We have presented simulations of a collapsing massive protostellar core with an initially weak magnetic field. We have shown how the combined action of compression and gravitational instability amplify the weak initial field to produce a strong, dynamically important field in the resulting protostellar disk. Through a magnetic bouyancy instability, the field is able to permeate the low-density region above and below the disk, eventually producing magnetically driven bubbles that carry away small amounts of material from the disk to the low-density envelope.

References

Abel, T., Bryan, G. L., & Norman, M. L. 2002, The Formation of the First Star in the Universe, Science, 295, 93, http://adsabs.harvard.edu/abs/2002Sci...295...93A

Bate, M. R., Bonnell, I. A., & Price, N. M. 1995, Modelling accretion in protobinary systems, MNRAS, 277, 362, http://adsabs.harvard.edu/cgi-bin/nph-bib_query?bibcode=1995MNRAS.277..362B&db_key=AST

Biermann, L. 1950, Über den Ursprung der Magnetfelder auf Sternen und im interstellaren Raum (miteinem Anhang von A. Schlüter), Zeitschrift Naturforschung Teil A, 5, 65, http://adsabs.harvard.edu/abs/1950ZNatA...5...65B

Carilli, C. L., & Taylor, G. B. 2002, Cluster Magnetic Fields, ARA&A, 40, 319, http://adsabs.harvard.edu/abs/2002ARA

Clark, P. C., Glover, S. C. O., Klessen, R. S., & Bromm, V. 2011, Gravitational Fragmentation in Turbulent Primordial Gas and the Initial Mass Function of Population III Stars, ApJ, 727, 110, http://adsabs.harvard.edu/abs/2011ApJ...727..110C

Crutcher, R. M. 1999, Magnetic Fields in Molecular Clouds: Observations Confront Theory, ApJ, 520, 706, http://adsabs.harvard.edu/cgi-bin/nph-bib_query?bibcode=1999ApJ...520..706C&db_key=AST

Federrath, C., Banerjee, R., Clark, P. C., & Klessen, R. S. 2010, Modeling Collapse and Accretion in Turbulent Gas Clouds: Implementation and Comparison of Sink Particles in AMR and SPH, ApJ, 713, 269, http://adsabs.harvard.edu/abs/2010ApJ...713..269F

Federrath, C., Sur, S., Schleicher, D. R. G., Banerjee, R., & Klessen, R. S. 2011, A New Jeans Resolution Criterion for (M)HD Simulations of Self-gravitating Gas: Application to Magnetic Field Amplification by Gravity-driven Turbulence, ApJ, 731, 62, http://adsabs.harvard.edu/abs/2011ApJ...731...62F

Fryxell, B., et al. 2000, FLASH: An Adaptive Mesh Hydrodynamics Code for Modeling Astrophysical Thermonuclear Flashes, ApJS, 131, 273, http://adsabs.harvard.edu/abs/2000ApJS..131..273F

Kratter, K. M., Matzner, C. D., Krumholz, M. R., & Klein, R. I. 2010, On the Role of Disks in the Formation of Stellar Systems: A Numerical Parameter Study of Rapid Accretion, ApJ, 708, 1585, http://adsabs.harvard.edu/abs/2010ApJ...708.1585K

Krumholz, M. R., McKee, C. F., & Klein, R. I. 2004, Embedding Lagrangian Sink Particles in Eulerian Grids, ApJ, 611, 399, http://adsabs.harvard.edu/abs/2004ApJ...611..399K

Mellon, R. R., & Li, Z.-Y. 2008, Magnetic Braking and Protostellar Disk Formation: The Ideal MHD Limit, ApJ, 681, 1356, http://adsabs.harvard.edu/abs/2008ApJ...681.1356M

—. 2009, Magnetic Braking and Protostellar Disk Formation: Ambipolar Diffusion, ApJ, 698, 922, http://adsabs.harvard.edu/abs/2009ApJ...698..922M

Sur, S., Schleicher, D. R. G., Banerjee, R., Federrath, C., & Klessen, R. S. 2010, The Generation of Strong Magnetic Fields During the Formation of the First Stars, ApJ, 721, L134, http://adsabs.harvard.edu/abs/2010ApJ...721L.134S

Truelove, J. K., Klein, R. I., McKee, C. F., Holliman, J. H., Howell, L. H., & Greenough, J. A. 1997, The Jeans Condition: A New Constraint on Spatial Resolution in Simulations of Isothermal Self-gravitational Hydrodynamics, ApJ, 489, L179+, http://adsabs.harvard.edu/cgi-bin/nph-bib_query?bibcode=1997ApJ...489L.179T&db_key=AST

Xu, H., O'Shea, B. W., Collins, D. C., Norman, M. L., Li, H., & Li, S. 2008, The Biermann Battery in Cosmological MHD Simulations of Population III Star Formation, ApJ, 688, L57, http://adsabs.harvard.edu/abs/2008ApJ...688L..57X

Yoshida, N., Omukai, K., & Hernquist, L. 2008, Protostar Formation in the Early Universe, Science, 321, 669, http://adsabs.harvard.edu/abs/2008Sci...321..669Y